Settling Velocity of Particles in a Grid-Generated Turbulence

Harada, Masayoshi
Institute of Tropical Agriculture, Kyushu University

Hiramatsu, Kazuaki
Laboratory of Land-Drainage and Reclamation Engineering, Faculty of Agriculture, Kyushu University

Hayashi, Shizuo
Institute of Tropical Agriculture, Kyushu University

https://doi.org/10.5109/24341

出版情報：九州大学大学院農学研究院紀要. 44 (3/4), pp.385-402, 2000-02. Kyushu University
バージョン：
権利関係：

J. Fac. Agr., Kyushu Univ., **44** (3·4), 385–402 (2000)

Settling Velocity of Particles in a Grid-Generated Turbulence

Masayoshi Harada, Kazuaki Hiramatsu* and Shizuo Hayashi

Institute of Tropical Agriculture, Kyushu University 13, 6–10–1 Hakozaki,
Higashi–ku, Fukuoka 812–8581, Japan
(Received October 29, 1999 and accepted November 5, 1999)

The purpose of this study is to examine the retardation of the settling velocity of a particle in the turbulent flow generated by an oscillating grid through a numerical simulation and a hydraulic experiment. First, we measured trajectories of glass beads in a grid–generated turbulence to verify the validity of the numerical simulation for particle behavior. Next, we examined the dynamic response of particles utilizing wavelet analysis and the relationship between the retardation of the mean settling velocity and the turbulent characteristic. As a result, we could identify low–frequency components that particles would easily follow, and high frequency components that would affect the motion of particles in vertical fluid velocity fluctuations, respectively. Furthermore, it was found that the retardation of the mean settling velocity depends on the spectral distribution of high–frequency, and that the retardation rates increase with increases in turbulent intensity.

INTRODUCTION

In the study on the convection diffusion phenomena of a suspension of particles in a turbulent shear flow, it is essential that the retardation of settling velocities is examined through the average and dynamic responses of a particle to the turbulence. Harada *et al.* (1997) estimated vertical profiles of turbulent diffusion coefficients and settling velocities from a diffusion equation and a concentration distribution of suspended kaolin in an open channel flow. They suggested that the settling velocities were affected by high–frequency components in vertical fluid velocity fluctuations. Hiramatsu *et al.* (1999) studied the trajectories and terminal settling velocities of kaolin floc in vertical and horizontal oscillating flows modeled on a sine–wave by numerical simulations, and concluded that the mechanism of the retardation of settling velocities was similar to the results obtained for sand particles in other studies previously presented. Harada *et al.* (1999) examined properties of settling velocities of kaolin floc in 2–dimensional turbulent shear flows generated by the Monte–Carlo simulation, using probabilistic and statistical knowledge of turbulent structures in open channel flows. They grasped the relationship between the motion of floc and vertical velocity fluctuations utilizing wavelet analysis, and found dimensionless parameters prescribing the retardation rates of mean settling velocities.

Baird *et al.* (1967), Tunstall and Houghton (1968) and Ikeda *et al.* (1988) clarified experimentally that values of settling velocities of spheres in sinusoidally oscillating fluids were smaller than ones in stationary fluids. Especially, Murray (1970) examined the retardation of the settling velocity of a sphere in the fluid generated by an oscillating grid.

* Laboratory of Land–Drainage and Reclamation Engineering, Faculty of Agriculture, Kyushu University 46–05, Fukuoka, 812–8581, Japan

Although past experimental studies on the behavior of particles have treated flows having properties which were simplistic and uniform in the vertical direction, there have been few reports about actual flows that have vertical profiles of turbulent properties.

In this study, trajectories of glass beads were measured in the region where turbulent intensities vertically varied in the turbulent flow generated by an oscillating grid, and their behaviors were reproduced by numerical simulation utilizing the nonlinear Lagrangian momentum equation. We verified the validity of this numerical simulation by comparing numerical solutions and measuring results, and furthermore, examined the average and dynamic response of particles in the grid-generated turbulence. In other words, the purpose of this study was to examine the retardation of the settling velocities in oscillating fluid of which probabilistic and statistical properties varied spatially through the hydraulic experiment and numerical simulation.

HYDRAULIC EXPERIMENT

Experimental Apparatus

Experiments were carried out in a colorless and transparent acrylic tank of water, 29 cm square by 100 cm deep, as sketched in Fig. 1. The stirrer employed was a grid made of steel wires 0.3 mm in diameter having a mesh size of M_s=0.1 cm. This grid, connected to a motor and two cams by two oscillating rods and two supporting rods to move steadily up and down in a vertical line, was placed 29 cm above the bottom of the tank. A styrene form was mounted over the water surface in order to prevent turbulence generated by waves formed on the surface. The grid was oscillated vertically with the

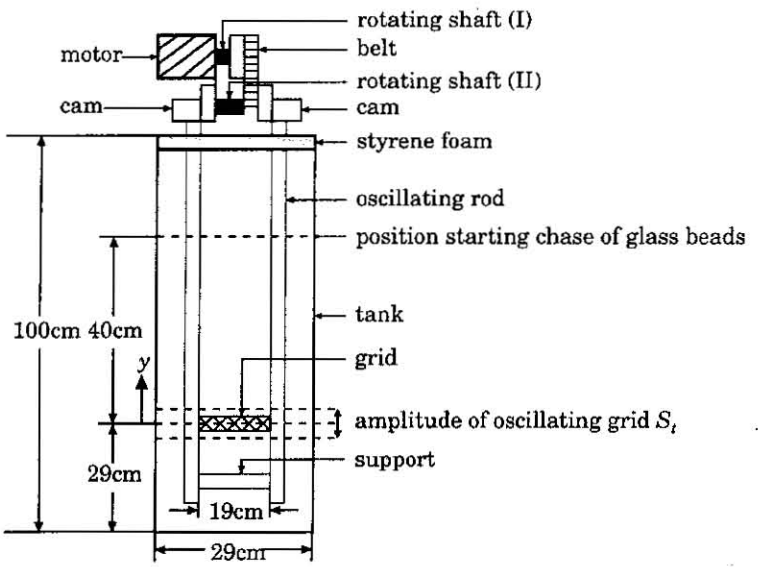

Fig. 1. A sketch of the experimental tank with the oscillating grid.

stroke as S_t=1.25 cm and stirrer frequencies as f_o=11, 21, 30 Hz. The vertical coordinate in the tank takes a positive upward direction from the middle of the oscillating amplitude, and characteristics of the grid-generated turbulence and trajectories of glass beads were respectively measured in the range of y=2 cm to y=40 cm.

Grid-generated Turbulence

Grid-generated turbulence is the flow produced by oscillating a grid horizontally placed in a stationary fluid, and has properties such that the turbulent characteristics are homogeneous in horizontal planes and vary with distance from the grid, and the mean velocity is zero. Characteristics of grid-generated turbulence has been quantitatively evaluated in studies such as entrainment and mixing across a density interface (Turner, 1968; Thompson and Turner, 1975; Hopfinger and Toly, 1976; Ura *et al.*, 1984). Since an oscillating fluid with a large turbulence was required when examining the settling velocity of particles, the apparatus and conditions for the oscillating grid used in this study were a little different from ones in conventional studies. Thereby we grasped the turbulent characteristics such as turbulent intensity and the power spectrum of velocity fluctuations.

Grid-generated turbulence can be divided into two regions. One corresponds to the region in which the grid moves up and down, where there is a generation of uniform turbulence in the vertical direction. The other is equivalent to the region of the top position of the grid to the water surface, where the turbulence decays with distance away from the grid. Since the amplitude of the oscillating grid was as small as S_t=1.25 cm, particles settled primarily in the region where the turbulence decayed in measurements of particle trajectories. So, this section addresses turbulent properties in that region. Velocity fluctuations of horizontal and vertical components were measured at intervals of 3 cm utilizing the Laser Doppler Anemometer, and the sampling frequency of data and the number of data were 200 Hz and 8192, respectively. In the section, turbulent characteristics such as the turbulent intensity and power spectrum in the vertical direction are described because we deal with particle motion in grid-generated turbulence as a one-dimensional phenomenon, such that only vertical fluid velocity fluctuations act on a particle.

(1) Vertical Profiles of Turbulent Intensity

Fig. 2 shows vertical profiles of mean flow velocities V and turbulent intensities v' in the vertical direction. From this figure, it is found that values of mean flow velocities were nearly zero, $V \approx 0$, in the range of $y \geq 15$ cm, but V became a little larger in proximity to the grid. Also, it is found that the values of v' decreased as the distance from grid y was increased in the range of $y \leq 20$ cm, and that there was the tendency such that v' increased in the range of $y > 20$ cm. It is considered that these results were attributed to the following factors; 1) the turbulence was an unsteady state, because the amount of turbulent kinetic energy supplied from the oscillating grid was small in the range of $y >$ 20 cm, 2) new currents were produced by oscillating rods, and 3) there was the generation of weak circulating currents from the effect of the side wall.

Vertical profiles of turbulent intensities are determined by external parameters such as stirring frequency f_o, stroke S_t and mesh size M_s. Then, referring to the result of the

dimensional analysis obtained by Sekine *et al.* (1985), the regression equation for the turbulent intensity v' is given as the following;

$$\frac{v'}{f_o S_t} = \alpha_v \cdot \left(\frac{S_t M_s f_o}{\nu} \right)^{\beta_v} \cdot \left(\frac{y}{M_s} \right)^{\gamma_v} \tag{1}$$

where ν is the kinematic viscosity of water. The measuring section was divided into 2 cm

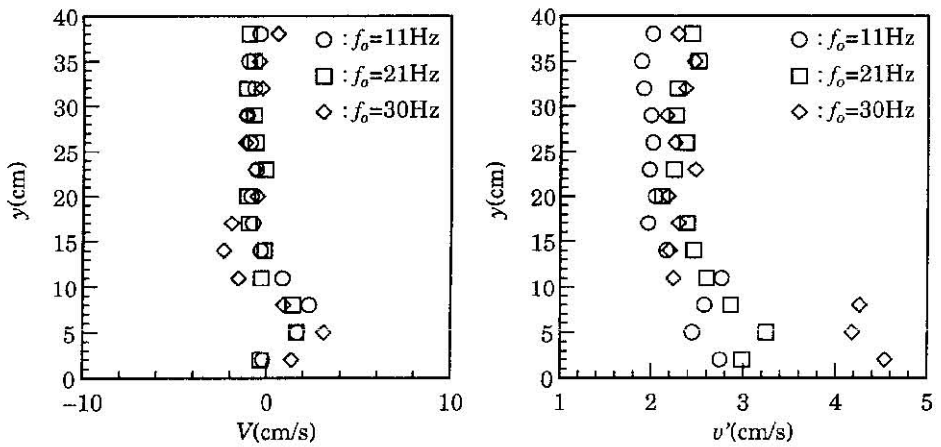

Fig. 2. Vertical profiles of mean flow velocities V and turbulent intensities v' in the vertical direction.

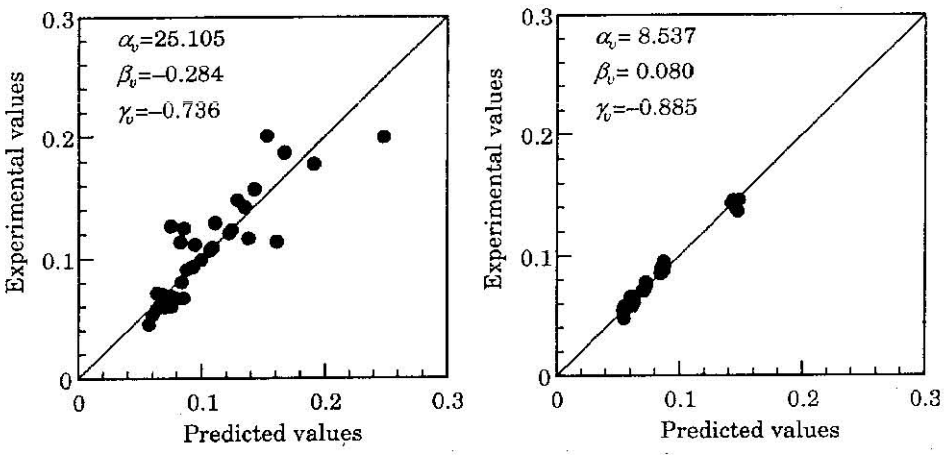

Fig. 3. Scatter plots of predicted and measured turbulent intensities (left: 2 cm$\leq y \leq$20 cm, right: 20 cm$< y \leq$40 cm).

$\leq y$ 20 cm and 20 cm$<y\leq$40 cm in consideration of the results in Fig. 2, and coefficients of the regression equations (1) were determined for each range. These values are shown in Fig. 3. The predicted values agreed with the experimental results, so we could predict turbulent intensities in the region where the turbulence decays from equation (1).

(2) Power Spectrum of Velocity Fluctuations

Fig. 4 shows power spectrum $P_{v0}(f)$, which was obtained by normalizing the frequency spectrum calculated from the vertical velocity fluctuations using the FFT method by its corresponding turbulent intensity, at y=2, 11, 29, 38 cm. Comparing the power spectra of each measuring point at one stirring frequency, it is found that the contribution of high-frequency components to the mean square power v'^2 increased with regression of y, that is, the spectral distributions were not similar in the vertical direction. Also, Fig. 4

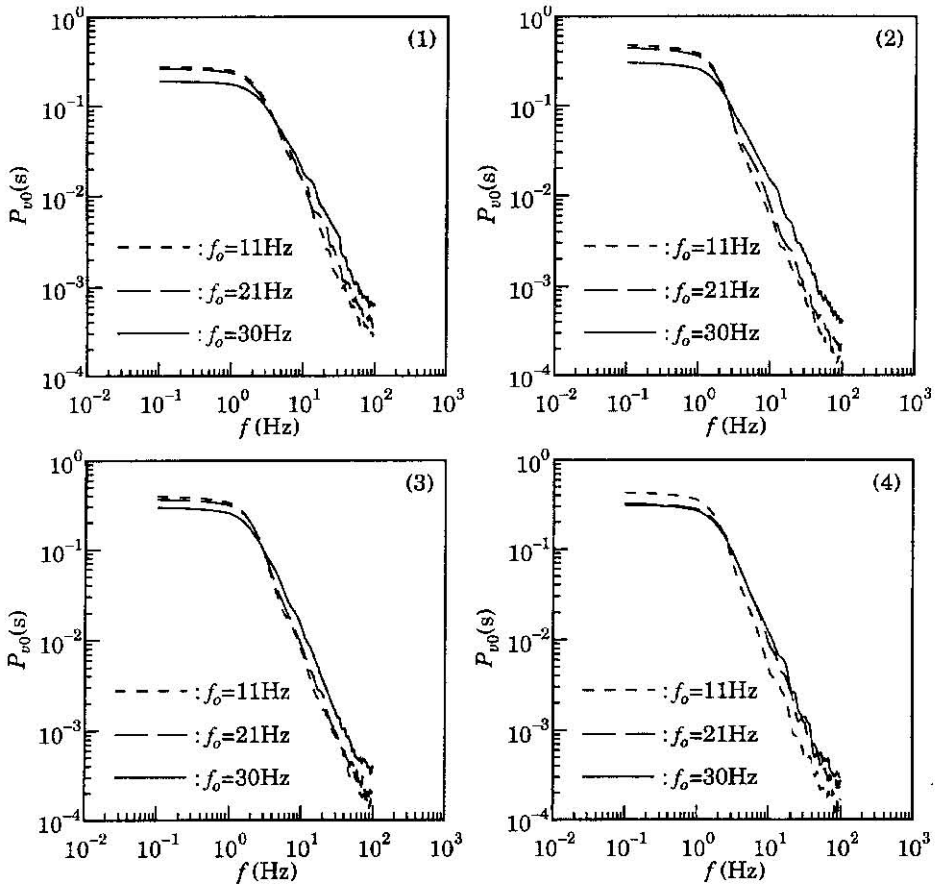

Fig. 4. Variations of normalized power spectrum of vertical velocity fluctuations with y and f_o ((1)y=2.0 cm, (2)y=11.0 cm, (3)y=29.0cm, (4)y=38.0 cm).

shows that the contribution of high-frequency components at the same position increased with frequency f_o. In summary, the grid-generated turbulence in this study had the property such that the contribution rate of the energy in the high-frequency range to mean square energy varied for the vertical coordinate and condition of stirring frequency.

Measurement of Particle Trajectory

In this section, the trajectories of particles in the grid-generated turbulence having the turbulent characteristic described above were experimentally grasped. The particles used in the hydraulic experiment were glass beads of the specific gravity 2.5, and it was confirmed that their shape was almost spherical by microscopic photographs. Ranges of particle diameter were distinguished by sifting glass beads, and the measurements of their trajectories were carried out for three cases as shown in Table 1. Symbols d and w_0 in Table 1 are the representative diameter and terminal settling velocity in stationary fluid, respectively.

Table 1. Experimental conditions of particle

	Ranges of particle diameter (cm)	d (cm)	w_0 (cm/s)
Case1	0.0500～0.0600	0.0500	9.810
Case2	0.0180～0.0212	0.0196	2.557
Case3	0.0090～0.0100	0.0095	0.736

Trajectories of particles were measured utilizing a potentiometer – a circular resister probing the rotational angle from a change in electric resistance –. By applying a voltage of 3 V to the potentiometer, equipped with a pulley 11.83 cm in diameter through a steel wire, the output signals from the resister were taken in through an AD-converter. After injecting glass beads into the water tank, we pulled the wire while conforming the motion of the particle visually. By converting an amount of change in the voltage from the potentiometer to a moved distance of the wire, we could obtain the trajectory of beads in a grid-generated turbulence.

The trace was carried out by shining a laser beam from a laser diode placed to emit light horizontally at the objective particle in order to minimize measuring errors. Also, slit light was shone on the upside of the water surface to keep the object in sight. Since it was difficult to trace the particle visually for Case3, the process of particle sedimentation was recorded on video at intervals of 10 cm, and the trajectory was measured using video images.

The plural measurements stated above for one case were implemented to minimize measuring errors, and this experimental data was averaged. So, the objected trajectory meant the averaged behavior of a particle in one grid-generated turbulence. All results of the measurements are depicted in Fig. 5 with trajectories in stationary fluids calculated from w_0 shown in Table 1. From this figure, it was found that the mean settling velocity through the objective section was smaller than the one in the stationary fluid as frequency f_o increased, and that the retardation was remarkable in the range of $y \leq 20$ cm where the turbulent intensity was relatively large.

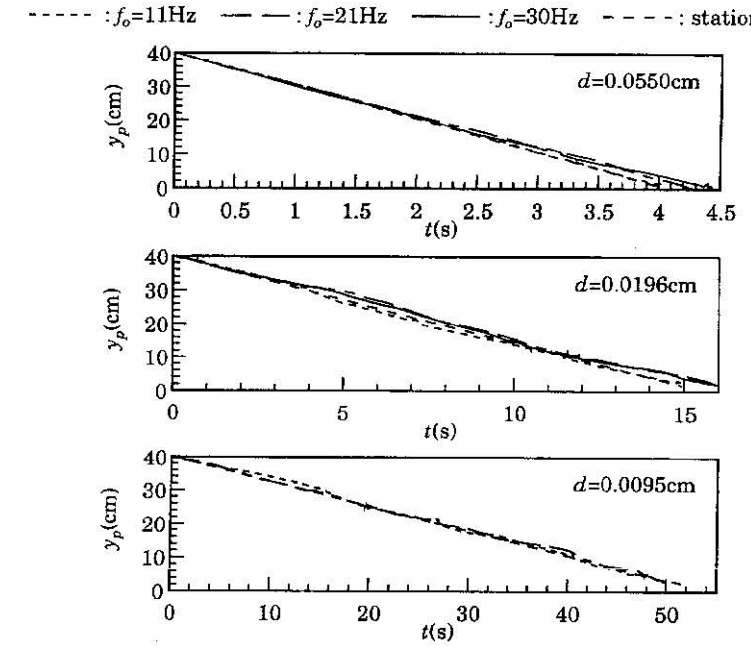

Fig. 5. Trajectories of glass beads in the grid-generated turbulence and the stationary fluid.

NUMERICAL SIMULATION

Nonlinear Lagrangian Momentum Equation

The vertical forces governing particle motion in turbulent flows are fluid pressure gradient, submerge weight of the particle, drag force and the force due to added mass effect. In the vertical direction y taking a positive upward direction, the resulting governing equation becomes (Hinze, 1959),

$$\frac{dv_p}{dt} = \frac{3C_D\rho_f}{4d(\rho_p+C_m\rho_f)}|v_p-v_f|(v_p-v_f) + \frac{(1+C_m)\rho_f}{\rho_p+C_m\rho_f}\frac{dv_f}{dt} - \frac{\rho_p-\rho_f}{\rho_p+C_m\rho_f}g \qquad (2)$$

in which subscripts f and p represent physical quantities for fluid and solid particles, respectively; v is the vertical velocity, C_D is the drag coefficient, C_m is the added mass coefficient which is equal to 0.5 for a sphere, ρ is the density and g is the gravitational acceleration. In equation (2), the Basset term, which takes into account the effect of the deviation in a flow pattern from its steady state, was neglected to reduce the calculating time because it could be considered that there was no effect of the Basset term on calculating results (Sekine and Kikkawa, 1987; Ikeda *et al.*, 1988; Yamasaka *et al.*, 1990; Gotoh *et al.*, 1995). Drag coefficient C_D was treated as a function of the particle Reynolds

number R_{ep} using the relative particle speed, and given by the following;

$$C_D = \frac{24}{R_{ep}} + \frac{3}{\sqrt{R_{ep}}} + 0.34,\ R_{ep} = \frac{|v_f - v_p|\,d}{\nu} \tag{3}$$

The above equation is applicable to the entire region of the particle Reynolds number for a sphere.

Numerical Simulation of Fluid Velocity Fluctuations

The velocity fluctuations in the grid-generated turbulence were duplicated utilizing the power spectrum shown in Fig. 4, that is, they were simulated by synthesizing sine-waves considering the ration of each frequency component determined by the spectral distribution. The fluid velocity fluctuations in the vertical direction, $v_f(t, y)$, given the spectrum $F_v(f, y)$, can be reproduced by the following;

$$\left.\begin{aligned} v_f(t,y) &= \sum_{k=1}^{N} \sqrt{2F_v(\overline{f_k}, y)\,\Delta f_k}\cos\left(2\pi\overline{f_k}\,t + \theta_k\right) \\ \overline{f_k} &= \left(f_k + f_{k-1}\right)/2,\ \Delta f_k = f_k - f_{k-1},\ \theta_k = 2\pi\,\xi_0 \end{aligned}\right\} \tag{4}$$

where f_k is the discrete frequency, ξ_0 is the uniform random number of [0,1] and N is the number of frequencies dividing the spectrum. The frequency step for the discreteness of the spectral distribution, Δf, was 0.1 Hz, and the frequency range of 0.1 Hz to 100 Hz was divided up into one hundred equal-length elements. The time series of velocity fluctuations, $v_f(t, y)$, obtained from equation (4) are repeated in the maximum period $T(=1/\Delta f)=10$ s, and their average values are zero. Although mean flow velocities, V, were not zero in proximity to the grid as in Fig. 2, values of V were not considered in equation (4) for the following reasons; 1) experimental values of V were averaged for a long time, and 2) fluid velocities required in the numerical simulation were instantaneous values. An example of a time series of velocity fluctuations is shown in Fig. 6.

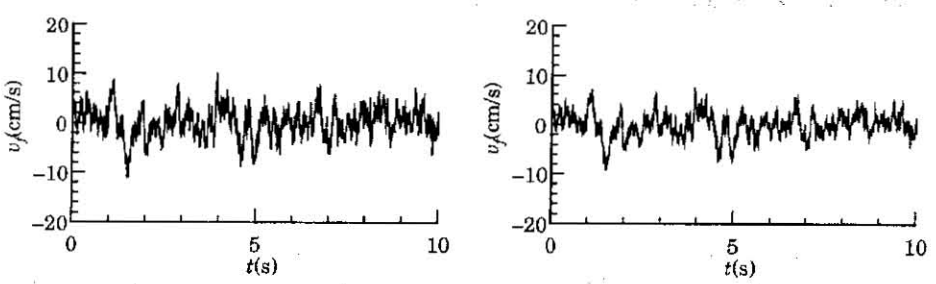

Fig. 6. Time series of vertical fluctuating velocities in the grid-generated turbulence calculated by equation (4) (f_c=21 Hz, left: y=2.0 cm, right: y=38.0 cm).

Numerical Solutions for a Basic Equation

An example of calculated results obtained by solving equation (2) with the

Runge–Kutta–Gill method is shown in Fig. 7, in which v_p is the absolute particle speed in the vertical direction, y_p is the trajectory of a particle, v_f is the fluid velocity in the neighborhood of the settling particle and V_p ($\equiv v_f - v_p$) is the velocity of a particle relative to the fluid, which is defined as the instantaneous settling velocity. Since trajectories obtained in the hydraulic experiments stated above denote the average behavior of a

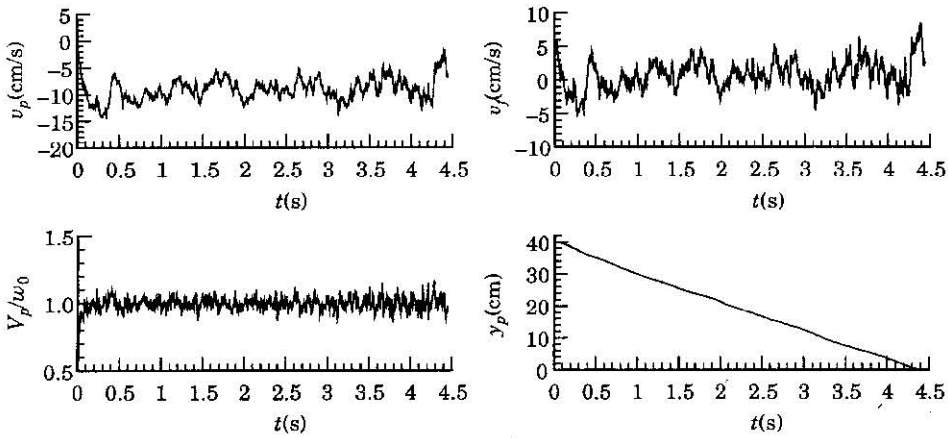

Fig. 7. An example of calculated results (d=0.055 cm, f_c=21 Hz).

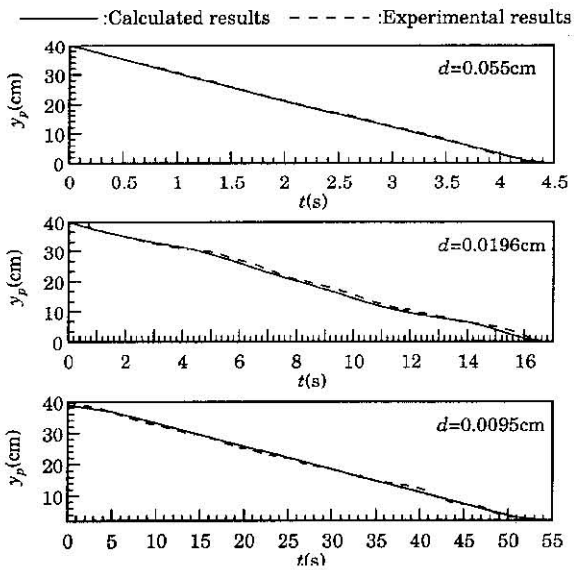

Fig. 8. Comparison of experimental results with calculated results (f_c=21 Hz).

particle, we needed to average values of y_p to compare calculated results to experimental results. So, we carried out 50 Lagrangian chases for one particle and one grid-generated turbulence, and calculated the ensemble mean of the trajectory, $E[y_p]$. Fig. 8 shows an example of $E[y_p]$ with the experimental results of trajectory corresponding to these calculating conditions. The calculated results agreed approximately with the experimental results, so it is found that the validity of the numerical simulation using equation (2) was verified.

RESULTS AND DISCUSSION

Dynamic Response of a Particle by Wavelet Analysis

Since the grid-generated turbulence in this study had vertical profiles of turbulent intensities as in Fig. 2, and spectral distributions of their velocity fluctuations varied with location as in Fig. 4, the probabilistic and statistical features of turbulent velocities acting on a particle changed every moment by the settling of the particle. Therefore, the time-frequency analysis, which can grasp temporal and spatial transitions of a signal simultaneously, is acquired for the analysis of dynamic response. Then we used the wavelet analysis – one of time-frequency analysis characterizing the signal by being able to associate various frequency bands with different time intervals – to examine the response of particles with the calculated results shown in Fig. 7. Wavelet analysis has the property such that it is able to extract the distribution of fluctuations of various time scales from the signal without losing the information for an original time axis, and is the ideal tool to use when attempting to analysis and characterize localized phenomenon in a signal.

(1) Wavelet Analysis

When an arbitrary time series, $G(t)$, is sampled at equal intervals over $0 \leq t < 1$, the orthogonal wavelet expansion for $G(t)$ is defined by the mother wavelet $W(t)$ as the following equation (Newland, 1993; Mori and Yasuda, 1996),

$$G(t) = \sum_j \sum_k a_{2^j+k} W_{j,k}(t) \quad (0 \leq t < 1) \tag{5}$$

where t is the independent variable divided by the signal over duration T, $W_{j,k}(t)$ is the wavelet, and a_{2^j+k} is the wavelet coefficient. Wavelets $W_{j,k}(t)$ are obtained by transforming mother wavelet $W(t)$ with scale parameter j and location parameter k as the following;

$$W_{j,k}(t) = 2^{j/2} W\left(2^j t - k\right). \tag{6}$$

Wavelets $W_{j,k}(t)$ are the functions that represent the local appearance in a time series, and makes it possible to analyze $G(t)$ on the time-frequency plane. Defining $g_i(t) = \sum_k 2^{j/2} a_{2^j+k} W(2^j t - k)$, the wavelet expansion of equation (5) can be revised as the following;

$$G(t) = g_{-1}(t) + g_0(t) + g_1(t) + \cdots + g_j(t) + \cdots. \tag{7}$$

The above equation shows that the wavelet transform can resolve the signal into its

constituent parts – wavelet components $g_j(t)$ –. Each wavelet component represented by index j is called a 'level', and these levels are numbered from −1 upwards. Integer k covers the number of wavelets in each level. In a discrete wavelet transform, the number of data M determines how many wavelet levels there are, that is, when $M=2^m$ there are $m+1$ wavelet levels. At the level $j(\neq -1)$, there are 2^j wavelets each spaced $M/2^m$ apart along the t-axis. Therefore, k takes the range of 0 to 2^j-1. The wavelet coefficients a_{2^j+k} give the amplitudes of each of the contributing wavelets $W_{j,k}(t)$. For example, a_0 is the amplitude of the scaling function, and a_1, (a_2, a_3) and (a_4, a_5, a_6, a_7) are the amplitudes of wavelet functions at level 0, 1 and 2, respectively. The typical frequency (central frequency) $f_{c,j}$ of each level is defined as follows ,

$$f_{c,j} = 2^j \cdot \frac{f_s}{2^m} \quad (j=0, 1, \cdots, m-1) \tag{8}$$

where f_s is the sampling frequency of data. Level −1 has no wavelets, and represents the mean value of data.

The mother wavelet, corresponding to the basis in the Fourier transform, forms the building block – basis function – into which the signal can be decomposed, and the shape of the wavelet components depends on $W(t)$. This study utilized Daubechies' wavelet, D20, as the orthogonal mother wavelet. This wavelet has 12 vanishing moments, and thus is very smooth. Also, Daubechies' wavelet is thought to be useful for a process that exhibits considerable variability at all scales (Venugopal and Foufoula-Georgious, 1996). When using this wavelet, the wavelet coefficients can be easily calculated by Mallat's tree algorithm (Newland, 1993).

Considering the orthogonality of wavelets and the conservation of area, the mean-square value of $G(t)$ can be calculated by squaring both sides of the equation obtained by substituting (6) into (5) and integrating over $0 \leq t < 1$ as the following (Newland, 1993),

$$\int_0^1 G^2(t)\,\mathrm{d}t = a_0^2 + \sum_j \sum_k 2^{-j} \cdot a_{2^j+k}^2 . \tag{9}$$

Equation (9) shows how the mean-square of $G(t)$ is distributed between different wavelet levels and between different wavelets within each level. It is considered from this equation that a wavelet coefficient squared, a_i^2, represents the energy to the square power of each wavelet component at its corresponding level and position.

(2) Time-frequency Analysis of Fluid Velocity Fluctuations

The time-frequency analysis of v_y shown in Fig. 7 was carried out by wavelet analysis to examine localized properties of velocity fluctuations acting on a particle. Fig. 9 shows an example of the time-frequency-energy plots of wavelet components for v_y. This figure indicates the distributions of the energy values, a_i^2, plotted on the time-frequency plane taking the transversal axis as time t and taking the longitudinal axis as central frequency f_c. Here, since the sampling frequency of data was 200 Hz, the maximum frequency was 100 Hz. From Fig. 9, it is easily found that contributions of frequency bands for the mean square of v_y varied with time, especially energy values of high-frequency components increased as time proceeds as the particle approached the oscillating grid. Also, it is

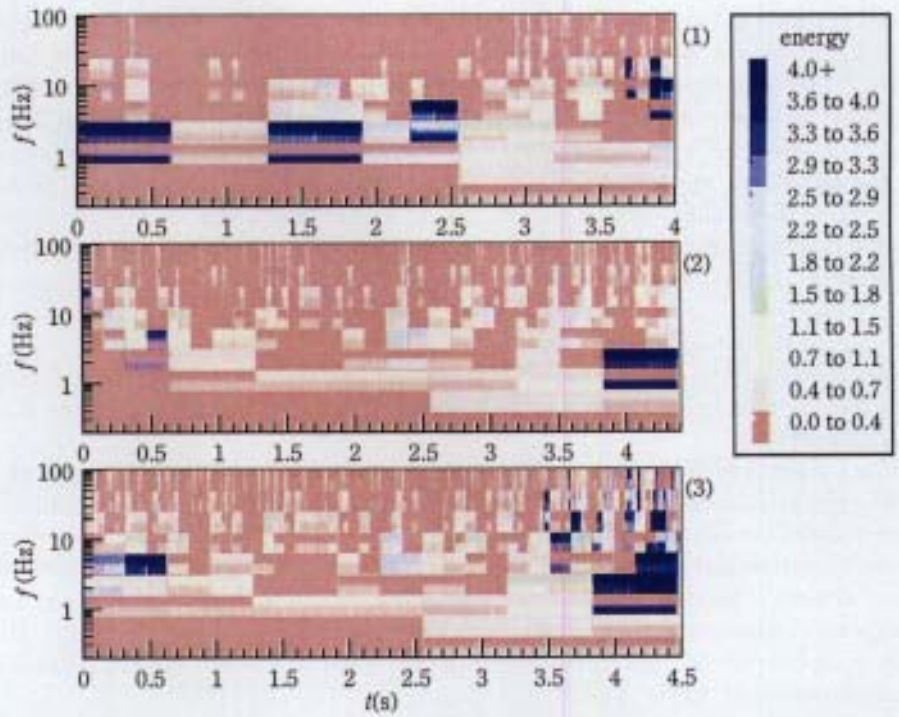

Fig. 9. Variations of time–frequency–energy plots for v_f with f_s (d=0.055 cm, (1) f_s=11 Hz, (2) f_s=21 Hz, (3) f_s=30 Hz).

found that contributions of high–frequency bands became large as the stirring frequency f_s was large. Comparing Fig. 9 to Fig. 5, it is considered that retardation of settling velocities on the range close to the grid, $y \leq 10$ cm, was associated with increases of the energy of high–frequency bands.

(3) Relations between Particle Motion and Fluid Velocity Fluctuations

In the study on the settling velocities of spheres in oscillating fluids, it is concluded that a particle's drop is dominated forcefully by low–frequency components of fluid velocity fluctuations, and the retardation of terminal settling velocities is due to high–frequency components which cause the negative result of particles following the fluid (Gotoh *et al.*, 1994; Nakagawa *et al.*, 1994; Gotoh *et al.*, 1995). Then we examined the relationship between particles' motion and fluid velocity fluctuations by the wavelet decomposition of v_f in this section.

Fig. 10 indicates wavelet components of v_f shown in Fig. 7. Since the number of data $M=2^{10}$, there were 11 wavelet levels. We evaluated cross–correlation coefficients, $C_{vv}(\tau)$, between wavelets components of v_f and the particle velocity v_p to find out what variation components of v_f particles easily followed, and an example of these results is shown in Fig. 11. It was found from this figure that there were no correlations between

high-frequency components and particle velocity, and that v_p was correlated with low-frequency components of 1.563 Hz to 6.25 Hz and the value of $C_{vf}(\tau)$ was largest at f_c=1.563 Hz. That is, the particle in this case easily followed the low-frequency component of f_c=1.563 Hz. Then we defined the central frequency of the wavelet component where the value of $C_{vf}(\tau)$ was maximum at $\bar{f}_L$, and the results of all cases are shown in Table 2. Table 2 indicates that the period of the fluctuation component dominating a particle's motion becomes longer in keeping with particle diameter d.

Fig. 12 shows an example of the relationship between the ratio of the instantaneous settling velocity in a grid-generated turbulence to the terminal settling velocity for a stationary fluid, V_p/w_0, and the energy, a_j^2, of wavelet coefficients for v_f. From this figure it is found that fluctuations of V_p/w_0 became large as increases of energy of wavelet components went over f_c=12.5 Hz or f_c=25 Hz, and that the relations V_p/w_0 and a_j^2 were unclear in the low-frequency range. From these results it may be inferred that fluctuation components over one frequency have an effect on the instantaneous settling velocities. Then we defined this boundary frequency as f_H, and results of all cases are shown in Table 2. Allowing for the results of Gotoh *et al.* (1994), Nakagawa *et al.* (1994) and Gotoh *et al.* (1995), it is considered that high-frequency components over f_H shown in Table 2 caused the negative result of particles following the fluid.

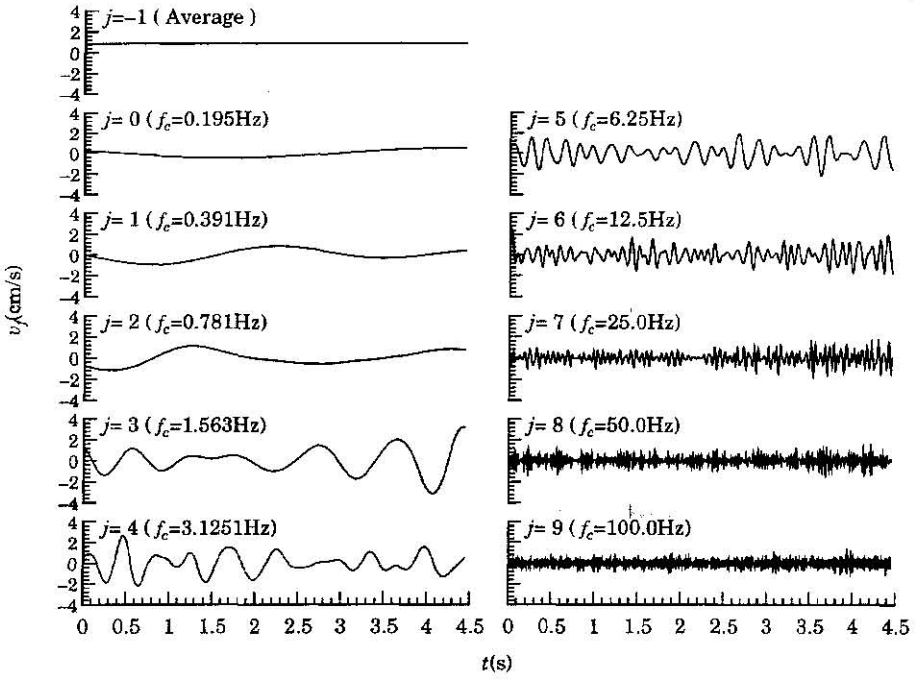

Fig. 10. Wavelet components of v_f (d=0.055 cm, f_s=21 Hz).

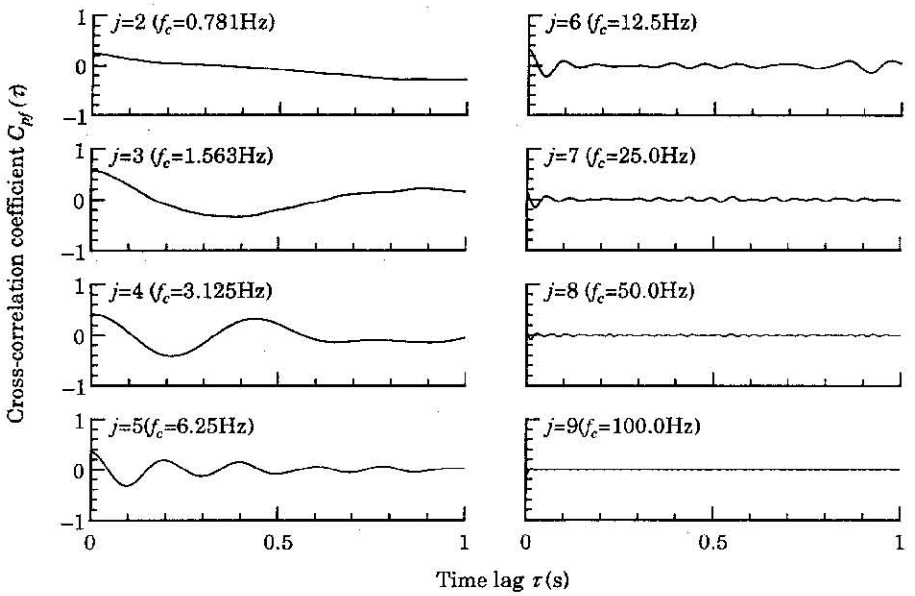

Fig. 11. Cross-correlation coefficients between wavelet components of v_f and v_p (d=0.055 cm, f_c=21 Hz).

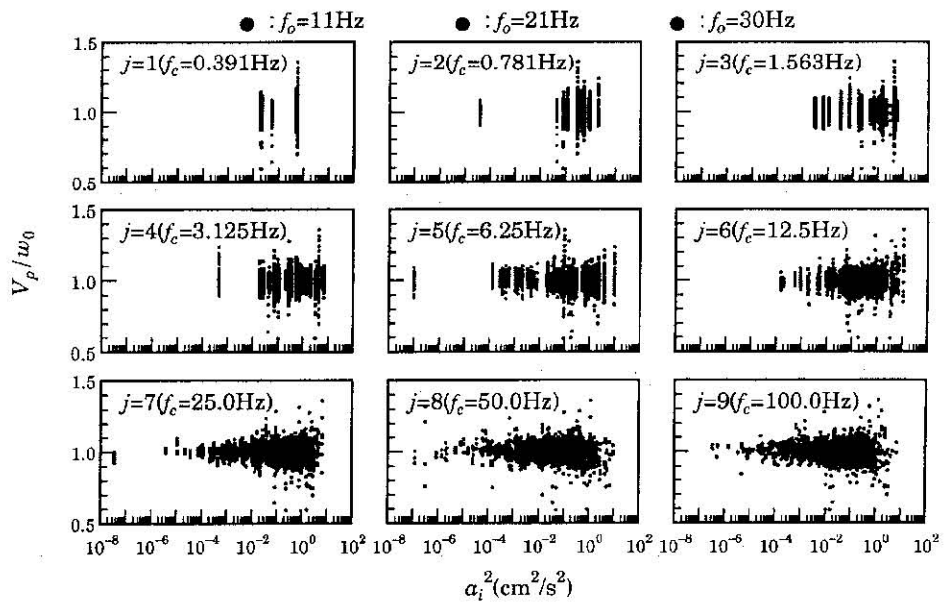

Fig. 12. Relationships between V_p/w_0 and a_i^2 (d=0.055 cm).

Table 2. Values of f_l and f_h of each particle diameter

Particle diameter d(cm)	Low-frequency f_l(Hz)	High-frequency f_h(Hz)
0.0550	1.563	12.5
0.0196	3.125	25.0
0.0095	6.250	50.0

Mean Settling Velocity and Turbulent Intensity

This section states variation of the mean settling velocity, w_p, in a grid-generated turbulence. Vertical profiles of w_p were estimated by the following. First, 50 numerical simulations were carried out for one calculation condition, and ensemble means of $V_p(=v_f-v_p)$ were calculated. Next, moving averages, 2s for Case1, 5s for Case2 and 10s for Case3, were executed for these ensemble means $E[V_p]$, and we defined this value as the mean settling velocity w_p. Also, the averaged trajectory Y_p was estimated the same way. Fig. 13 shows an example of variations of w_p and Y_p, and we can obtain vertical profiles of the mean settling velocity by corresponding w_p and Y_p.

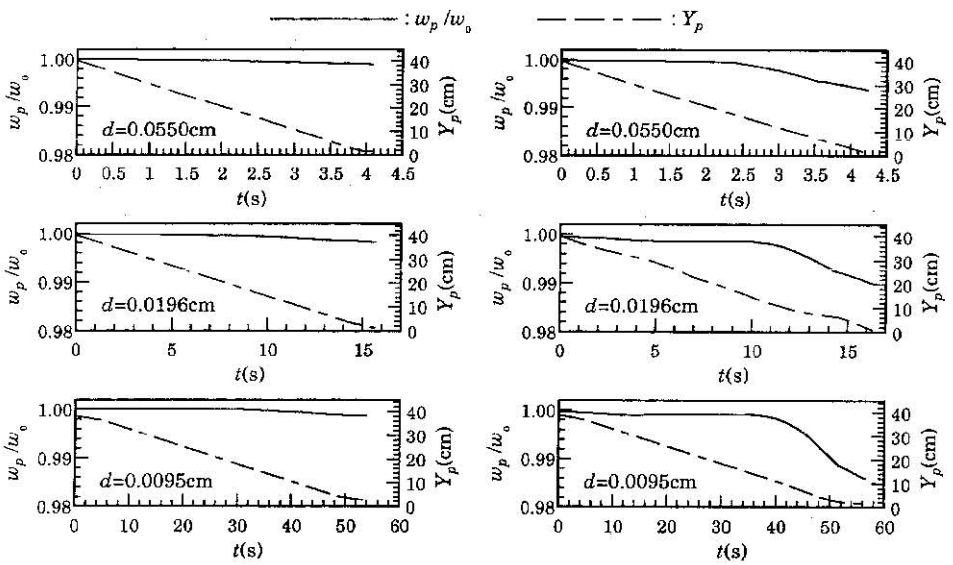

Fig. 13. Variations of the mean setting velocity w_p and the averaged trajectory Y_p with t (left: f_c=11 Hz, right: f_c=30 Hz)

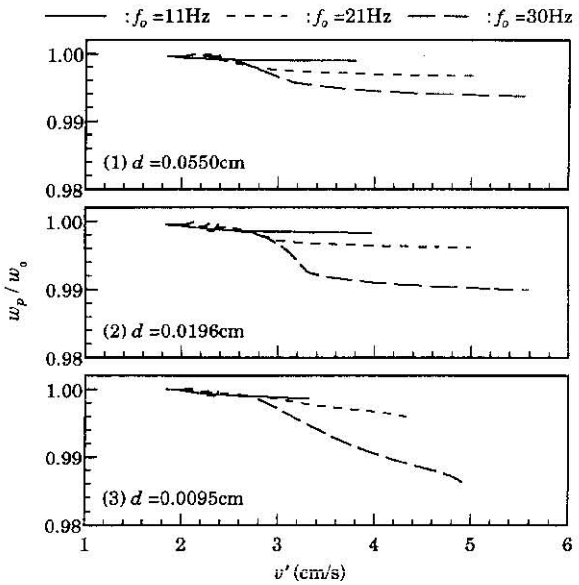

Fig. 14. Relationships between the mean settling velocity w_p and the turbulent intensity v'.

Fig. 14 shows a relationship between w_p/w_0 and turbulent intensity v' at their corresponding positions. Values of v' were calculated by substituting Y_p into regression equation (1). From Fig. 14 it is found that mean settling velocities decreased with increasing v', and that the amount of retardation of settling velocities became large with increasing f_c when comparing w_p/w_0 at the same turbulent intensity. It is considered that this result was ascribed to the turbulent property such that the rate of contribution of power in the high-frequency range to the mean square power, v'^2, became larger in keeping with the stirring frequency f_c. That is, retardation of the mean settling velocity is dominated by the power of high-frequency components, as in Fig. 12 and Table 2, in fluid velocity fluctuations acting on particles, and the amount of retardation increases with the turbulent intensity.

CONCLUSIONS

The objective of this study was to examine the dynamic response of particles and the retardation of the settling velocity in a grid-generated turbulence by a numerical simulation by which its validity was verified through the hydraulic experiment for particle trajectory.

The results obtained are summarized as follows

1. From cross-correlation coefficients between particle velocity and wavelet components for fluid velocity fluctuations acting on a particle, a particle can easily follow the

low-frequency component of f_l, as shown in Table 2.

2. From the relationship between the instantaneous settling velocity and the energy of wavelet components for fluid velocity fluctuation, the high-frequency components over f_H shown in Table 2 arose from the negative result of particles following the fluid.
3. The retardation of the settling velocity depended on the contribution variable power of the high-frequency range to mean square power of velocity fluctuations, and the amount of that increased with increasing turbulent intensity.

ACKNOWLEDGEMENTS

The authors wish to thank Dr. Shiomi Sikasho and Dr. Ken Mori (Laboratory of Land—Drainage and Reclamation Engineering, Faculty of Agriculture, Kyushu University) for many helpful suggestions.

REFERENCES

Baird, M. H. I., M. G. Senior and R. J. Thompson 1967 Terminal velocities of spherical particles in a vertically oscillating liquid. *Chemical Engineering Science*, **22**: 551–557

Gotoh, H., T. Tsujimoto and H. Nakagawa 1994 Dynamics of Suspended Particle in Vertical Random Oscillating Flow. *Proceedings of Hydraulic Engineering, Japan Society of Civil Engineers*, **38**: 585–590 (in Japanese with English summaty)

Gotoh, H., T. Tsujimoto and H. Nakagawa 1995 Time Scale of Sediment Suspension in Fluid with Vertical Random Oscillations. *Proceedings of Japan Society of Civil Engineers*, **515**(II-31): 67–76 (in Japanese with English summaty)

Harada, M., K. Hiramatsu, S. Shikasho and K. Mori 1997 A Method of Concentration Measurement using Image Processing to Estimate Turbulent Diffusion Coefficient and Particle Fall Velocity for Suspended Kaolin in Open Channel Flow. *Transactions of the Japanese Society of Irrigation, Drainage and Reclamation Engineering*, **192**: 95–104 (in Japanese with English summaty)

Harada, M., K. Hiramatsu, S. Shikasho and K. Mori 1999 Wavelet Analysis of Dynamic Response of Floc in Turbulent Shear Flows – Settling Velocity of Floc in Turbulent Flows (II)–. *Transactions of the Japanese Society of Irrigation, Drainage and Reclamation Engineering*, **201**: 309–316 (in Japanese with English summaty)

Hinze, J. O. 1959 *Turbulence–An Introduction to Its Mechanism and Theory*. McGraw-Hill Book Company Inc.: 352–364

Hiramatsu, K., S. Shikasho and K. Mori and M. Harada 1999 Retardation of Settling Velocity in Simusoidally Oscillating Flows – Settling Velocity of Floc in Turbulent Flows (I)–. *Transactions of the Japanese Society of Irrigation, Drainage and Reclamation Engineering*, **200**: 179–187 (in Japanese with English summaty)

Hopfinger, E. J. and J. A. Toly 1976 Spatially decaying turbulence and its relation to mixing across density interfaces. *Journal of Fluid Mechanics*, **78**: 155–175

Ikeda, S., M. Yamasaka, K. Kiuchi and H. Takahashi 1988 Fall Velocity of Spheres in Vertically Oscillating Fluid. *Proceedings of Japan Society of Civil Engineers*, **393**(II-9): 57–66 (in Japanese with English summaty)

Mori, N. and T. Yasuda 1996 Nonlinear Characteristics of Random Wave Train by Wavelet Analysis. *Proceedings of Japan Society of Civil Engineers*, **533**(II-34): 157–169 (in Japanese with English summaty)

Murray, S. P. 1970 Settling Velocities and Vertical Diffusion of Particles in Turbulent Water. *Journal of Geophysical Research*, **75**(9): 1647–1654

Nakagawa, H., T. Tsujimoto, H. Gotoh and Y. Inoue 1994 Energy Spectrum–Based Simulation of Turbulence and Its Application to Stochastic Model of Suspension. *Proceedings of Hydraulic Engineering, Japan Society of Civil Engineers*, **38**: 591–596 (in Japanese with English summaty)

Newland, D. E. 1993 *An introduction to random vibrations, spectral and wavelet analysis.*

Longman Scientific and Technical: 295–370

Sekine, M., M. Hirosue, S. Kikuchi and H. Kikkawa 1985 Study on the Mechanism of Suspended Load. *Proceedings of Japanese Conference on Hydraulics*, **29**: 503–508 (in Japanese with English summaty)

Thompson, S. M. and J. S. Turner 1975 Mixing across an interface due to turbulence generated by an oscillating grid. *Journal of Fluid Mechanics*, **67**: 349–368

Tunstall, E. B. and G. Houghton 1968 Retardation of falling spheres by hydrodynamic oscillations. *Chemical Engineering Science*, **23**: 1067–1081

Turner, J. S. 1968 The influence of molecular diffusivity on turbulent entrainment across a density interface. *Journal of Fluid Mechanics*, **33**: 639–656

Ura, M., T. Komatsu and N. Matsunaga 1984 Interfacial Properties and Entrainment due to Turbulence Generated by an Oscillating Grid. *Proceedings of Japan Society of Civil Engineers*, **345**(II-1): 91–99 (in Japanese with English summaty)

Venugopal, V. and E. Foufoula-Georgiou 1996 Energy decomposition of rainfall in the time–frequency–scale domain using wavelet packets. *Journal of Hydrology*, **187**: 3–27

Yamasaka, M. and S. Ikeda 1990 Theoretical Study on Mean Fall Velocity of Spheres in Fluids with Vertical Random Oscillations. *Proceedings of Japan Society of Civil Engineers*, **417**(II-13): 173–179 (in Japanese with English summaty)